HYDROLOGICAL PROCESSES
Hydrol. Process. **26**, 741–759 (2012)
Published online 24 June 2011 in Wiley Online Library
(wileyonlinelibrary.com) DOI: 10.1002/hyp.8176

A temperature-precipitation-based model of thirty-year mean snowpack accumulation and melt in Oregon, USA†

Scott G. Leibowitz,* Parker J. Wigington Jr., Randy L. Comeleo and Joseph L. Ebersole
US Environmental Protection Agency, National Health and Environmental Effects Research Laboratory, Western Ecology Division, Corvallis, OR 97333, USA

Abstract:

High-resolution, spatially extensive climate grids can be useful in regional hydrologic applications. However, in regions where precipitation is dominated by snow, snowmelt models are often used to account for timing and magnitude of water delivery. We developed an empirical, nonlinear model to estimate 30-year means of monthly snowpack and snowmelt throughout Oregon. Precipitation and temperature for the period 1971–2000, derived from 400-m resolution PRISM data, and potential evapotranspiration (estimated from temperature and day length) drive the model. The model was calibrated using mean monthly data from 45 SNOTEL sites and accurately estimated snowpack at 25 validation sites: $R^2 = 0{\cdot}76$, Nash-Sutcliffe Efficiency (NSE) = 0·80. Calibrating it with data from all 70 SNOTEL sites gave somewhat better results ($R^2 = 0{\cdot}84$, NSE = 0·85). We separately applied the model to SNOTEL stations located <200 and ≥200 km from the Oregon coast, since they have different climatic conditions. The model performed equally well for both areas. We used the model to modify moisture surplus (precipitation minus potential evapotranspiration) to account for snowpack accumulation and snowmelt. The resulting values accurately reflect the shape and magnitude of runoff at a snow-dominated basin, with low winter values and a June peak. Our findings suggest that the model is robust with respect to different climatic conditions, and that it can be used to estimate potential runoff in snow-dominated basins. The model may allow high-resolution, regional hydrologic comparisons to be made across basins that are differentially affected by snowpack, and may prove useful for investigating regional hydrologic response to climate change. Published in 2011 by John Wiley & Sons, Ltd.

Additional Supporting information may be found in the online version of this article.

KEY WORDS snowpack; snowmelt; SWE; temperature index model; regional hydrology; hydrologic landscapes

Received 15 July 2010; Accepted 23 May 2011

INTRODUCTION

Regional hydrologic studies have benefitted from the availability of spatially extensive climate data that can be used to estimate components of the hydrologic cycle. Variables such as temperature and precipitation have been mapped nationally and globally on a 1-km grid at monthly and shorter time steps by interpolating data from ground-based meteorological stations (Thornton *et al*., 1997; Hijmans *et al*., 2005). In the United States, 30-year climate normals are available at finer spatial resolutions of 800 and even 400 m (Daly *et al*., 2008; http://www.climatesource.com/400_meter.html). Applications of such spatially extensive data include regional mapping of hydrologic characteristics (Church *et al*., 1995; Kolditz *et al*., 2007), hydrologic modelling to predict characteristics of streamflow (Vogel *et al*., 1999; Kroll *et al*., 2004; Santhi *et al*., 2008), and estimates of the potential impacts of climate change on water resources (Hamlet *et al*., 2005; Howat and Tulaczyk, 2005; Nolin and Daly, 2006).

Spatially extensive climate data are also valuable for the development of hydrologic classification systems (Wolock *et al*., 2004; Sobota *et al*., 2009; Hutchinson *et al*., 2010). An effective classification approach could allow hydrologic assessments to identify ungauged catchments or landscape units with similar hydrologic characteristics (McDonnell and Woods, 2004; Devito *et al*., 2005; Sivapalan, 2005). Classification approaches have been developed that use regression or multivariate techniques to relate landscape or watershed attributes to aspects of the hydrologic regime (Holmes *et al*., 2002; Sanborn and Bledsoe, 2006). Other classification approaches focus on the interactions of climate, geomorphology, and geology (Winter, 2001; Devito *et al*., 2005; Dahl *et al*., 2007). Winter (2001) recognized the need for broad-scale generalisations of hydrologic attributes and proposed the concept of hydrologic landscapes. The hydrologic landscape concept assumes that common behaviours of groundwater, surface water, and the interactions of the two with the atmosphere can be associated with different variations and multiples of fundamental hydrologic landscape units. Wolock *et al*. (2004) developed a national map of hydrologic landscape regions based on concepts from Winter (2001), using best available data on a 1-km grid. One limitation of the Wolock *et al*. (2004) approach is that it did

* Correspondence to: Scott G. Leibowitz, US Environmental Protection Agency NHEERL-WED, 200 SW 35th St, Corvallis, OR 97333, USA. E-mail: leibowitz.scott@epa.gov

not account for altered seasonality of moisture surplus (precipitation minus potential evapotranspiration) due to the accumulation and melt of snowpacks.

For regional hydrologic applications that use spatially extensive climate grids, precipitation data can be useful for representing annual hydrologic inputs. However, if timing of water delivery is of interest, then snow accumulation and snowmelt must be accounted for in mountainous areas where precipitation is dominated by snowfall. This is necessary because moisture surplus is generally stored during winter months and does not contribute to stream flow until the spring or summer. Thus, the issue of how to produce snowmelt data that can complement spatially extensive, high-resolution climate data is of interest. For example, as a part of our research into the effects of headwater streams and wetlands on larger rivers (Leibowitz *et al*., 2008), we have developed a hydrologic landscape (HL) classification for the State of Oregon (private communication, P.J. Wigington, Jr., US EPA Western Ecology Division, Corvallis, OR, 2 June 2011). This employs a direct classification approach using five indices related to expected hydrologic behaviour: annual climate, seasonality, aquifer permeability, terrain, and soil permeability. We are using these HLs for several broad-scale applications, including hydrologic classification, assessing stream flow duration, and estimating discharge at ungauged sites. Our work incorporates concepts and principles from Winter (2001) and Wolock *et al*. (2004), but includes a number of significant modifications. One of these changes was to incorporate an index of seasonality, which was defined as the season of maximum water availability based on mean monthly climate data. Because of its mid-latitude location and the influence of the Pacific Ocean, precipitation in Oregon is greatest during the winter (Taylor and Hannan, 1999). However, in the mountainous areas, this precipitation is mostly stored as snowpack, and does not become available until spring or summer snowmelt occurs. As a result, a snowmelt model was needed that could be used to estimate available water. Another change was to use 30-year (1971–2000) mean monthly climate data with a 400 m (0·16 km^2) spatial resolution. These are the highest resolution, spatially extensive climate data available in the US. While use of these data allows for analysis of very fine spatial patterns, a trade-off is the limited number of climate variables available: precipitation, temperature, and freeze dates (Daly *et al*., 2008; http://www.climatesource.com/400_meter.html). Thus, we specifically needed a model that could be applied to a large, spatially extensive area at high spatial resolution and which could be driven by a limited set of climate variables.

There are two main approaches to snowmelt modelling. Mechanistic energy balance models have been developed (Kustas *et al*., 1994; Albert and Krajeski, 1998; Cline *et al*., 1998; Adam *et al*., 2009; Singh *et al*., 2009) that simulate the physical processes involved in snowmelt. While these models include basic heat and water balances, different authors may emphasize different processes. For example, water flow through multiple snow layers *versus* a single layer (Albert and Krajeski, 1998), a one- *versus* two-layer soil column (Liang *et al*., 1994), and use of modelled *versus* satellite-derived albedo estimates (Molotch *et al*., 2004). By incorporating the physics that drive snowmelt—e.g. heat fluxes associated with net short- and long-wave radiation, latent heat, sensible heat, ground heat, and advected heat—these models can be used to predict behaviour outside the range of available observations and conditions. Energy balance models require a number of input variables that may include air temperature, wind speed, relative humidity, precipitation, solar and long-wave radiation, and ground heat flux. Because the availability of such detailed data is limited, energy balance models cannot be applied to broader areas without somehow estimating these meteorological data from other factors (Williams and Tarboton, 1999; Adam *et al*., 2009). One example of such an approach is the National Operational Hydrologic Remote Sensing Center Snow Model, which produces hourly snow analyses, including snow water equivalent (SWE), for the conterminous US at a 1-km resolution using gridded model estimates of solar and long-wave radiation, air temperature, precipitation, relative humidity, and wind speed (Carroll *et al*., 2006).

The second approach to snowmelt modelling is the temperature index method, which uses air temperature as an index for snowmelt. An example of this type of model is the degree-day approach, where the depth of snowmelt is calculated as the product of the number of degree-days above some threshold, a degree-day factor, and snow covered area (Martinec and Rango, 1986; Kustas *et al*., 1994; Fontaine *et al*., 2002; Molotch *et al*., 2004; Singh *et al*., 2009). These models have few parameters and input variables, and make use of generally available data (e.g. temperature, precipitation, and snow covered area). As a result, degree-day approaches have been applied broadly and over large areas. For example, the Snowmelt Runoff Model has been used in over 100 basins ranging in size from 0·8 to 917444 km^2 (Martinec *et al*., 2008). Other types of temperature index models have also been developed (e.g. Beschta, 1975; McCabe and Wolock, 1999). Because temperature index models employ an empirical approach, results may not be valid for extreme or unusual conditions (Cline *et al*., 1998) or if conditions or processes change from those that occurred during the period being analysed. Also, it may not be possible to apply such models to heterogeneous terrain or transfer results to basins with different climatic conditions (Williams and Tarboton, 1999).

Given our objective to develop high-resolution, statewide estimates of long-term, average monthly snowmelt for Oregon, an energy balance approach was not feasible, since this would require data that are limited in their distribution or spatial resolution. For example, data that drive the National Operational Hydrologic Remote

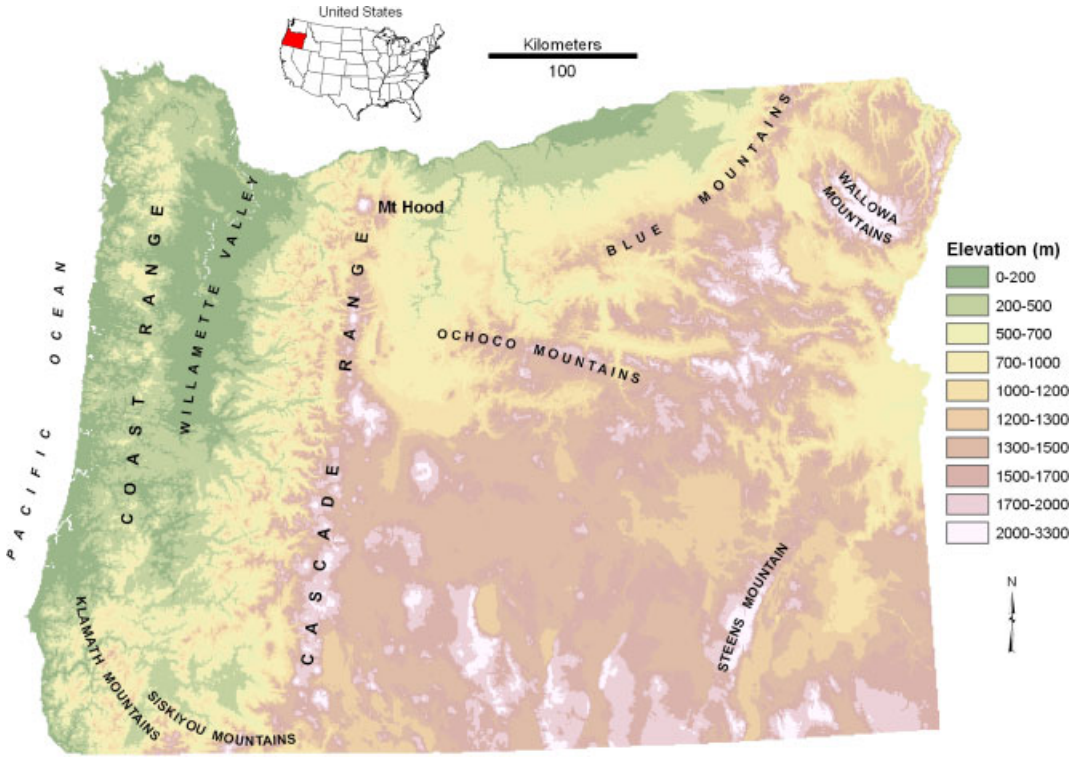

Figure 1. Elevation map of Oregon with major features

Sensing Center Snow Model are only available for a 1-km grid (Carroll *et al*., 2006). Therefore, we chose to use a temperature index method. Most temperature index approaches model daily time series, in contrast to the 30-year monthly normals we needed for our HL application. Thus, we decided to develop a simplified empirical model that uses temperature and precipitation data, along with calculated potential evapotranspiration, to produce high-resolution (400 m) estimates of average monthly snowpack accumulation and melt. The model's combination of high spatial resolution and long-term monthly averages could be useful in other applications, such as assessing hydrologic risk from global climate change.

METHODS

Study area

The State of Oregon is located in the northwestern United States, between 41°58′ and 46°16′ north latitude and 116°27′ and 124°34′ west longitude (Figure 1). Oregon has an area of 251165 km^2, and elevation ranges from sea level along the Pacific coast (the state's western border) to 3426 m at the peak of Mt Hood (Figure 1). Oregon's major topographic feature is the Cascade Mountain Range, which runs north–south and divides the state into western and central-eastern sections. Oregon has a number of other mountain ranges, including the Coast Range, the Klamath and Siskiyou Mountains to the southwest, the Wallowa and Blue Mountains in the northeast, Steens Mountain in the southeast, and the Ochoco Mountains in the state's centre (Figure 1). The Willamette Valley, home to the state's major population centres, is located between the Coast Range and the Cascades.

The state's major source of moisture is the Pacific Ocean. As a result, distance from the coast is one of the two major factors affecting the spatial distribution of precipitation, with the other being elevation (Taylor and Hannan, 1999; Figure 2). Because of the moisture-laden marine air and westerly winds, Oregon's major mountain ranges produce orographic precipitation to their west and rain shadows to their east. This is especially true for the Coast Range and Cascades, which are north–south running and located nearest the coast. The Cascades create a strong demarcation between the wet western third of the state and the dry eastern two thirds (Figure 2). Moisture conditions in western Oregon range from the moderately wet Willamette Valley (760–1520 mm average annual precipitation; Taylor and Hannan, 1999) to the wetter coastal areas (1780–2290 mm) and the very wet rain forests of the Coast Range (2540–5080 mm). In contrast, moisture conditions east of the Cascades are generally dry (200–380 mm) except at the higher mountains.

Elevation and distance from the coast are also the two greatest influences on the distribution of temperature across the state (Taylor and Hannan, 1999; Figure 3). Temperatures west of the Cascades are generally mild and, on the coast, relatively uniform, while temperatures on the east are more extreme. The more extreme eastern temperatures are due, in part, to the higher base elevations east of the Cascades (Figure 1).

Because of Oregon's mid-latitude coastal location, delivery of precipitation is greatest during the winter months (Figure 2). This results in a significant proportion

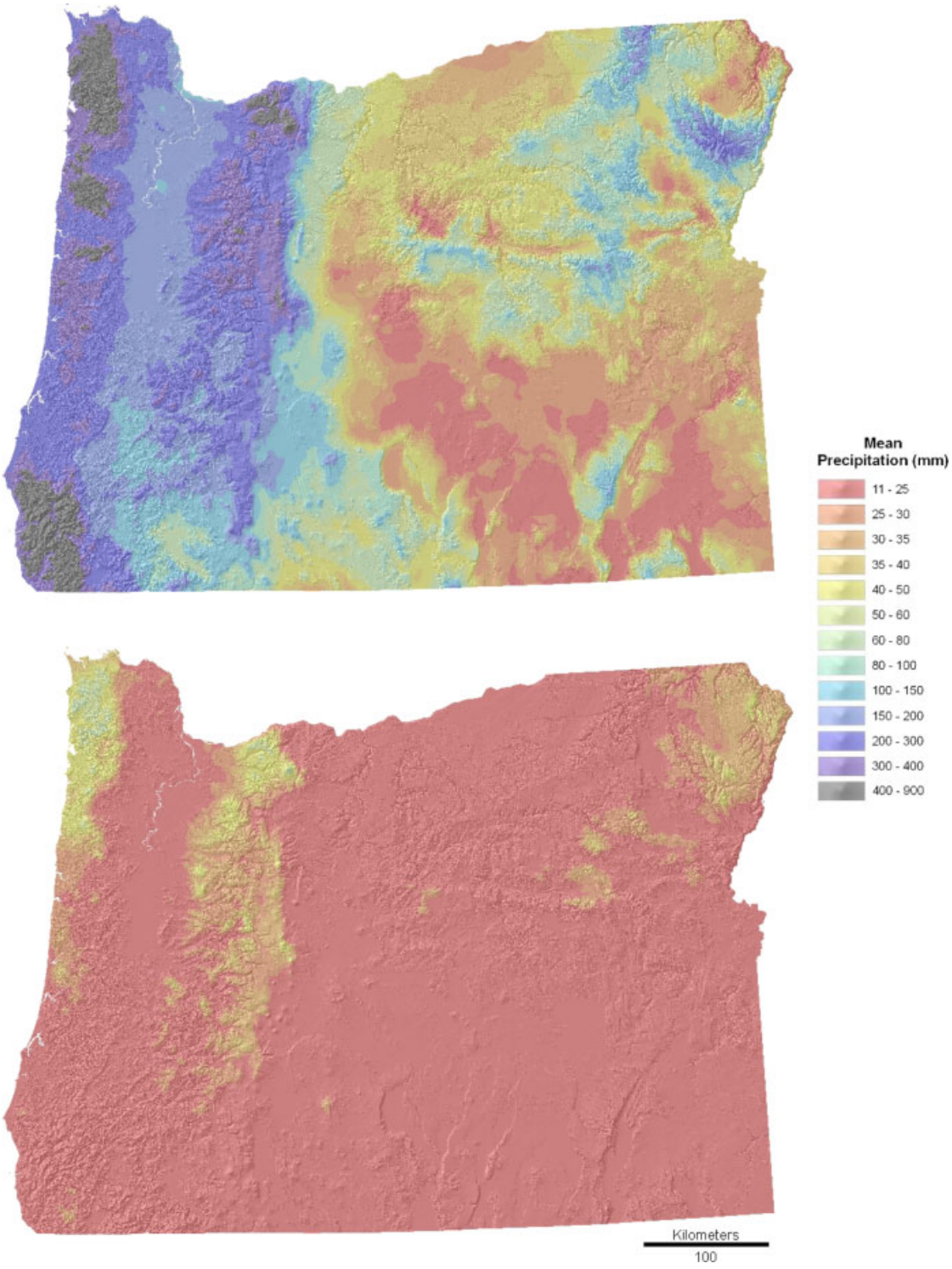

Figure 2. High resolution (400 m) PRISM data showing average (1971–2000) distribution of precipitation in Oregon for January (top) and July (bottom). Source: Climate Source, Inc

of Oregon's precipitation occurring as snow. For example, Serreze *et al*. (1999) estimated that 50 and 57% of annual precipitation falls as snow in the Pacific Northwest and Blue Mountains Regions, respectively. Although there is less overall precipitation east of the Cascades, snowfall can still be significant in the higher mountains (Figure 4). Because there are a number of peaks in the Wallowas with elevations greater than 2700 m, snowfall rates in this range can approach that of the Cascade peaks (Figures 1 and 4). Although the Coast Range has the highest precipitation rates in the state, it has relatively low snowfall (annual average of 25–76 mm; Ruffner, 1985) because of its lower elevation. The exceptions are higher elevation areas (Figure 4). Snowfall in the Willamette Valley is relatively low (Figures 1 and 4).

The diverse climatic conditions across Oregon are similar to those common to the US West. Oregon's western mountains and valleys are rain-dominated, much like

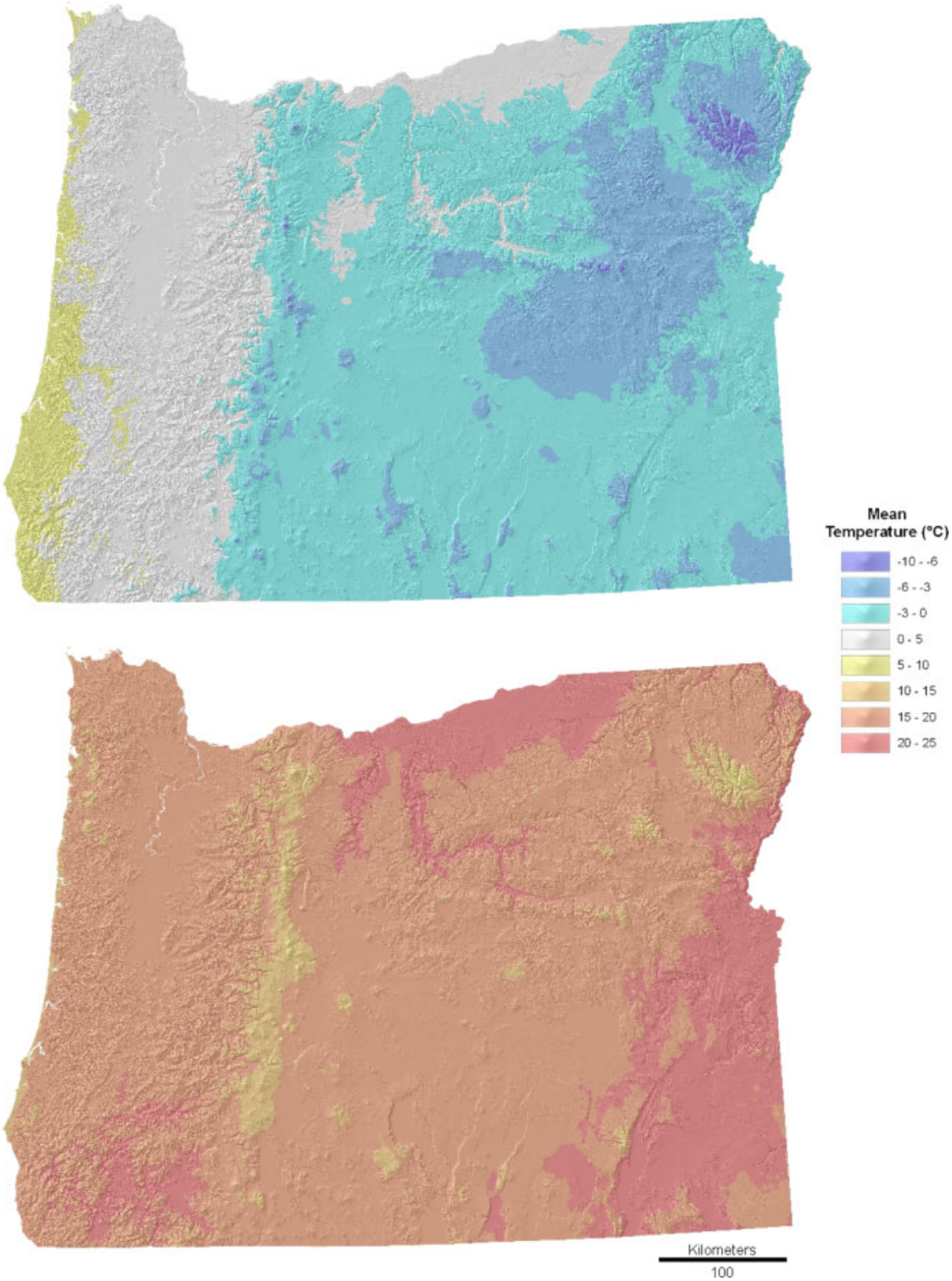

Figure 3. High resolution (400 m) PRISM data showing average (1971–2000) distribution of temperature in Oregon for January (top) and July (bottom). Source: Climate Source, Inc

western Washington and the northern coast of California. Conditions in Oregon's eastern mountains, particularly the Wallowa Mountains, are similar to climatic conditions in the Rocky Mountains. The dry semi-arid and arid basins have climatic characteristics found in the intermountain West (private communication, P.J. Wigington, Jr., US EPA Western Ecology Division, Corvallis, OR, 2 June 2011).

Studies that have examined temporal trends in snowpack provide insight into the effects of temperature and precipitation on snowpack. Numerous empirical and model-based studies have found strong evidence of negative temporal trends in snowpack within the western US, including Oregon (Hamlet *et al.*, 2005; Knowles *et al.*, 2006; Mote, 2006; Barnett *et al.*, 2008; Casola *et al.*, 2009; Grundstein and Mote, 2010). This includes not

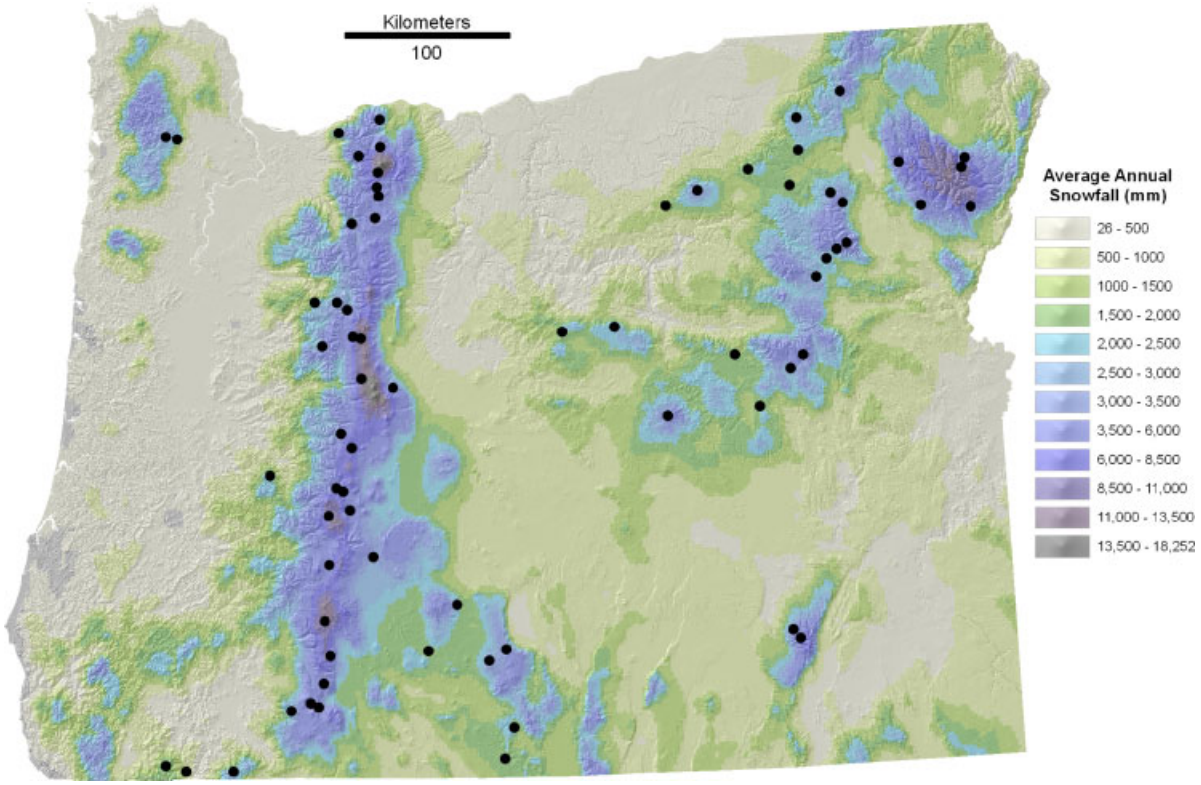

Figure 4. Map of Oregon showing location of 70 SNOTEL stations used in parameterising the models, overlaid on 30-year (1961–1990) average annual depth of freshly fallen snow (2 km grid size). Snowfall data from Climate Source, Inc

only declines in 1 April SWE, but also trends in earlier snow melt, earlier peak stream flows, and reduced stream flow. Trends in reduced snowpack have been attributed to both rising temperatures and decreasing precipitation. However, these two factors are differentially important at different locations. Increased temperatures, which have the dual effect of reducing the proportion of precipitation that occurs as snow and increasing the amount of snow melt, have a larger impact at lower elevations and on the Pacific coast, where temperatures are closer to freezing (Hamlet *et al*., 2005; Knowles *et al*., 2006; Mote, 2006; Grundstein and Mote, 2010). Higher elevation locations, such as the Sierra Nevada and the Rockies, are cold enough that warming trends have not impacted snowpack, and so temperature is less of a factor. Temporal trends in snowpack at these sites are more attributable to changes in precipitation (Hamlet *et al*., 2005; Mote, 2006).

Trends in temperature and precipitation are due in part to natural climate cycles, such as the Pacific Decadal Oscillation (PDO) and the North Pacific Index (NPI) (Hamlet *et al*., 2005; Knowles *et al*., 2006; Mote, 2006; Grundstein and Mote, 2010). However, these climate cycles are not sufficient to explain the negative snowpack trend. Long-term climate change is also considered a factor (Hamlet *et al*., 2005; Knowles *et al*., 2006; Mote, 2006; Barnett *et al*., 2008; Casola *et al*., 2009). For example, an analysis by Barnett *et al*. (2008) suggests that up to 60% of the trend in snowpack could be due to human-influenced climate change.

Model description

We use a nonlinear, mass balance approach to model average monthly snowpack. Specifically, the model uses a reverse S-shaped (inverted logistic) curve to represent the relationship between temperature and conversion of precipitation to snowpack. The rationale for using an S-shaped, rather than linear, function is that for a monthly time step conversion to snow should taper off, rather than completely cease, as average monthly temperature rises above freezing, since snow can fall on colder than average days. Other researchers have observed a similar, S-shaped relationship between temperature and various precipitation to snow indices (Auer, 1974; Beschta, 1975; Bartlett *et al*., 2006; Rutter *et al*., 2009). For the same reason, we use an S-shaped (logistic) curve to represent the effect of temperature on conversion of snowpack to snowmelt, since melting can occur during months with average temperatures below freezing on warmer than average days. Given that, we model snowpack depth as a function of the previous month's snowpack, snowpack accumulation, and snowmelt:

$$PACK_m = PACK_{m-1} + ACCUM_m - MELT_m \qquad (1)$$

where $PACK_m$ and $PACK_{m-1}$ are average monthly snowpack values at months m and $m-1$; $ACCUM_m$ is the net accumulation of new snowpack from moisture surplus during month m; and $MELT_m$ is loss of snowpack through conversion to snowmelt during month m. All terms are expressed as mm of SWE. Because $ACCUM_m$ is a net accumulation, it implicitly accounts for losses of

new snowpack due to melt or sublimation. However, we assume that all losses of old snowpack are due to melt ($MELT_m$), and that sublimation is negligible.

The accumulation term is calculated as a function of moisture surplus:

$$ACCUM_m = S_m \times p_{pack,m} = (P_m - PET_m) \times p_{pack,m} \quad (2)$$

where S_m is the monthly moisture surplus (mm), defined as the difference between precipitation (P_m) and potential evapotranspiration (PET_m); and $p_{pack,m}$ is a conversion efficiency that represents the net proportion of moisture surplus converted into snowpack during month m.

The conversion efficiency for snowpack formation is defined as a function of temperature using a two-parameter, inverted logistic function, so that a greater proportion of surplus is converted to snowpack as temperature decreases:

$$p_{pack,m} = 1 - \frac{1}{1 + e^{-(T_m + k_1)/k_2}} \quad (3)$$

where T_m is average monthly temperature (°C) and k_1 and k_2 are coefficients determined through calibration that control the left–right position and slope of the curve, respectively. Since $p_{pack,m}$ is a proportion it is unitless. Therefore, the units for k_1 and k_2 are °C.

The snowmelt term, $MELT_m$, is defined as a function of the previous month's snowpack:

$$MELT_m = PACK_{m-1} \times p_{melt,m} \quad (4)$$

where $p_{melt,m}$ is a conversion efficiency representing the net proportion of the previous month's snowpack converted into snowmelt during month m. This conversion efficiency is defined as a function of temperature using a two-parameter logistic function, so that a greater proportion of snowpack is converted to snowmelt as temperature increases:

$$p_{melt,m} = \frac{1}{1 + e^{-(T_m + k_3)/k_4}} \quad (5)$$

where k_3 and k_4 are coefficients determined through calibration that control the left–right position and slope of the curve, respectively, with units similar to k_1 and k_2. Note that while other temperature measures could be used in Equations (3) and (5) (e.g. T_{min} might be a better indicator of snowstorms that produce snowpack), we chose to take a parsimonious approach and use the same variable for both snowpack formation and snowmelt.

Because the snowmelt term does not include snowpack from the current month (Equation (4)), it might appear that snowpack would be overestimated by Equation (1). However, $ACCUM_m$ (Equation (2)) represents a net accumulation, since the model is fit to snowpack data (a net quantity), rather than gross snowfall. Thus, snowpack should not be overestimated.

Combining terms from Equations (1)–(5) gives the following expression for snowpack in month m:

$$\begin{aligned} PACK_m &= PACK_{m-1} + (P_m - PET_m) \times \left(1 - \frac{1}{1 + e^{-(T_m + k_1)/k_2}}\right) - PACK_{m-1} \frac{1}{1 + e^{-(T_m + k_3)/k_4}} \\ &= (P_m - PET_m)\left(1 - \frac{1}{1 + e^{-(T_m + k_1)/k_2}}\right) \\ &\quad + PACK_{m-1}\left(1 - \frac{1}{1 + e^{-(T_m + k_3)/k_4}}\right) \end{aligned} \quad (6)$$

Equation (6) models snowpack as a function of three input variables (P_m, PET_m, and T_m) and four parameters representing the left-right positions and slopes of the efficiency curves.

Independent variables

For P_m and T_m, we used gridded climate data derived using the PRISM (Parameter-elevation Regressions on Independent Slopes Model) algorithm (Daly *et al.*, 2008). Compared to other gridded climate data that are available for the entire conterminous US, PRISM data are available at a significantly greater spatial resolution: 400 m (0·16 km^2) grid cells (http://www.climatesource.com/400_meter.html) compared with 1-km grid cells for Daymet (Thornton *et al.*, 1997; http://www.daymet.org) or WorldClim (Hijmans *et al.*, 2005; http://www.worldclim.org). However, this greater spatial resolution comes with a trade-off: temporal resolution is monthly, compared to daily values for Daymet. In addition, 400-m PRISM data are only available as 30-year (1971–2000) averages. However, use of long-term averages at a high spatial resolution is appropriate for purposes of hydrologic classification, since the focus is on spatial (e.g. regional) comparisons, rather than annual variability.

The PRISM data were assembled from a large dataset of almost 13000 precipitation and 10000 temperature climate stations. At each grid cell, an individual regression is developed between a particular variable and elevation, using a minimum of 15 (temperature) or 40 (precipitation) climate stations. These stations are weighted to account for local topography and climate (Daly *et al.*, 2008). The regression is then used with the elevation at that cell to estimate the specific variable (e.g. average January precipitation). The 400 m (0·16 km^2) resolution datasets that we used (Figures 2–3) were derived from 800 m grids by using a Gaussian weighted filter (http://www.climatesource.com/us/fact_sheets/meta_precip_us_71b.html). PRISM data are available for purchase from Climate Source, Inc. (http://www.climatesource.com).

PET_m was calculated on the same 400 m grid as the PRISM data according to Hamon (1961):

$$PET_m = 13{\cdot}97 d_m D_{m,l}^2 W_m \quad (7)$$

where d_m is the number of days in month m; $D_{m,l}$ is the average day length for month m at latitude l, in units of 12 h; and W_m is the saturated water vapor density for the month in g m^{-3}.

$D_{m,l}$ was calculated by performing a first-order, linear trend interpolation between known day lengths (Lydolph, 1985) on the 15th day of the month at the 40th and 50th parallels. Saturated water vapour density is calculated (Hamon, 1961) as:

$$W_m = \frac{4{\cdot}95e^{0{\cdot}062T_m}}{100} \tag{8}$$

The Hamon (1961) approach has the advantage of only requiring air temperature measurements. This is critical to our current application, where high-resolution, statewide climate data are limited. Wolock *et al*. (2004) similarly used Hamon (1961) in a hydrologic classification application across the US. Although Hamon (1961) can produce biased results (Xu and Singh, 2001; Rosenberry *et al*., 2004), it is correlated with actual evapotranspiration at the watershed scale (Lu *et al*., 2005). Also, Hamon (1961) performs well compared with other approaches at multiple settings when used to predict PET as a component of hydrologic models (Oudin *et al*., 2005). By using Hamon (1961), we are able to drive our model with only three independent variables: precipitation, temperature, and latitude.

Response variable

In order to fit the model, we used data from the SNOwpack TELemetry (SNOWTEL) network to represent the response variable, $PACK_m$. SNOTEL is an automated system developed by the National Water and Climate Center (NWCC) of the US Dept. of Agriculture's Natural Resources Conservation Service. NWCC operates and maintains more than 750 SNOTEL stations in 13 western states and Alaska (NWCC, 2009). SNOTEL stations are located in remote, high-mountain watersheds and provide data on snowpack water content, snow depth, precipitation, and air temperature.

There are 78 active SNOTEL sites in the State of Oregon. Eight of the state's sites were not used in the analysis because data were missing or incomplete or because initial analyses indicated the site was an outlier. Average monthly snow water equivalent from the remaining 70 stations (Supporting Information I, Figure 4) were used to represent $PACK_m$. These data are derived using steel or hypalon pressure-sensing snow pillows (NWCC, 2009). There has been some suggestion that switching from steel to hypalon snow pillows at a site can cause a decrease of up to 25% in observed snow accumulation (Julander and Bricco, 2006; Julander 2007). However, we found no evidence of such a bias in an examination of 10 Oregon SNOTEL stations that had data from steel and hypalon pillows (Supporting Information II).

Thirty-year (1971–2000) averages for the 1st and 15th day of each month are provided by NWCC (http://www3.wcc.nrcs.usda.gov/nwcc/sweavg.jsp?state=OR). These averages are estimates, since none of the 70 stations were operating for this entire 30-year period. In fact, two of the stations were installed after 2000 (Supporting Information I). NWCC estimates the 30-year averages in one of two ways (ftp://ftp.wcc.nrcs.usda.gov/support/average/averages.pdf): using values from a nearly complete dataset with at least 25 years of data, or using data from a nearby, long-term snow course that is correlated (R^2 of at least 0·8) with the short-term record. In the latter case, the average is calculated using a combination of data from the actual station and estimates from the long-term snow course (private communication, J. Marron, National Water and Climate Center, Portland, OR, 22 July 2009). We then calculated the average monthly SWE for each site as the average of the values from the 1st and 15th of the month. Note that SNOTEL data are provisional and subject to revision; some minor changes in values have occurred since we downloaded the data on 4 January 2008. Although there are issues with SNOTEL data (see caveats section of discussion), they represent the best source of statewide data in Oregon and other western states.

Model fitting

The model was fit using monthly $PACK_m$ data from the SNOTEL stations as the dependent variable and P_m, PET_m, and T_m data (derived from the 400 m cell associated with each site) as the independent variables. We used the NLIN procedure under SAS 9·1 (SAS, 2003) to fit the model. NLIN estimates the parameters of a nonlinear model using the least squares method. We used the default Gauss-Newton method (SAS, 2003). The method is iterative, and we used the default value of 10^{-5} as the convergence criterion. Because NLIN is an iterative method, a starting value (or range of starting values) must be supplied for each parameter being estimated. For our runs, starting values for k_1 and k_3 (part of the numerator of the exponential terms in Equation (6)) ranged from -10 to 10 by 2. The ranges for k_2 and k_4 (the denominators of the exponential terms in Equation (6)) were 0·1 to 2·5 by 0·2.

We randomly selected 45 of the SNOTEL stations as calibration sites (Supporting Information I) that were used to fit an initial model with NLIN. We used this calibration model to sequentially calculate $PACK_m$ for each month beginning with October (the start of the water year), using an initial value of zero for $PACK_{SEPT}$. Note that by assuming snowpack is zero at the beginning of the water year our model excludes snowmelt from glacial sources. For each month, we restricted the calculated value of $PACK_m$ to a non-negative value, since SWE is a depth and cannot be negative. We then transformed the model output by using the intercept (β_0) and slope (β_1) of the regression between predicted *versus* observed SWE:

$$PACK_m{}^* = \max\left(0, \frac{PACK_m - \beta_0}{\beta_1}\right) \tag{9}$$

where $PACK_m{}^*$ is the transformed monthly snowpack value, restricted to a non-negative value. Note that the transformation occurs after all the monthly $PACK_m$ values are sequentially calculated; i.e. $PACK_m{}^*$ is calculated from $PACK_m$, and not from $PACK_{m-1}{}^*$. The corresponding transformed version of snowmelt is calculated as:

Table I. Parameter estimates and statistics for untransformed snowpack models

Model[a]	Parameter[b]	Estimate	Approx Std Error	Approx lower 95% CI[c]	Approx upper 95% CI[c]
Calibration	k_1	0·33	0·146	0·0455	0·6205
	k_2	1·90	0·182	1·5465	2·2605
	k_3	−8·05	0·085	−8·2146	−7·8809
	k_4	1·51	0·078	1·3553	1·6632
Combined	k_1	0·41	0·115	0·1854	0·6352
	k_2	1·86	0·141	1·5823	2·1371
	k_3	−8·04	0·070	−8·1800	−7·9061
	k_4	1·53	0·066	1·4041	1·6624

[a] Calibration model parameterized using monthly snowpack data from 45 randomly selected SNOTEL calibration sites (Supporting Information I); $n = 540$. Combined model parameterized with monthly snowpack data from complete set of 70 SNOTEL sites (Supporting Information I); $n = 840$.
[b] Model parameters as defined in Equation (6). Units for parameters k_1 through k_4 are °C.
[c] CI = Confidence Interval.

$$MELT_m{}^* = \begin{cases} -\Delta PACK_m{}^* = PACK_{m-1}{}^* - PACK_m{}^* \\ \qquad\qquad if\ PACK_{m-1}{}^* > PACK_m{}^* \\ 0 \qquad\qquad otherwise \end{cases} \quad (10)$$

We evaluated the transformed calibration model by calculating six statistics for $PACK_m{}^*$: R^2, Nash-Sutcliffe efficiency (NSE), root mean square error (RMSE), the ratio of the RMSE to the standard deviation (RMSE/STDDEV), the ratio of the RMSE to the range, and bias. The NSE compares model results with predictions based on the observed mean. The value ranges from $-\infty$ to 1, with a value of 1 for a perfect fit and negative values indicating that the model performs worse than use of the observed mean (Krause *et al.*, 2005).

We further assessed the transformed calibration model by determining how well it predicted snowpack at the 25 validation sites that were not used in the model parameterisation. This was evaluated with the same 6 statistics described above. We then re-estimated the 4 parameters of Equation (6) using the combined data from all 70 SNOTEL stations. We transformed this combined model using Equation (9), and then calculated the 6 evaluation statistics.

Finally, we separately evaluated the transformed, combined model for SNOTEL stations that were <200 and ≥200 km from the coast. We did this because several researchers have noted distinct patterns of snowpack in western Oregon (from the coast to the Cascades) compared to the eastern portion of the state (McCabe and Wolock, 1999; Serreze *et al.*, 1999). The Cascades have a maritime snow pattern with high snowfall and relatively warm winter temperatures (Nolin and Daly, 2006).

Statewide mapping

We used Equations (6) and (9) to calculate and map $PACK_m{}^*$ over the entire state using 400 m (0·16 km^2) gridded data. Values were calculated for each cell using monthly PRISM precipitation and temperature data (Figures 2 and 3) and the potential evapotranspiration values calculated from Equation (7). Analysis and mapping were done using ESRI's ArcGIS geographic information system software package in the Universal Transverse Mercator Zone 10 projection.

We also calculated modified monthly surplus ($S_m{}'$) over the entire state. This represents the average monthly amount of available (liquid) water:

$$S_m{}' = S_m - \Delta PACK_m{}^* = (P_m - PET_m) - \left(PACK_m{}^* - PACK_{m-1}{}^*\right) \quad (11)$$

If $\Delta PACK_m{}^* > 0$, then there is a net increase in snowpack (accumulation exceeds snowmelt), thereby reducing the amount of available water ($S_m{}' < S_m$). Conversely, if $\Delta PACK_m{}^* < 0$ the net decrease in snowpack causes a net release of water (output from snowmelt exceeds any conversion of precipitation into snowpack). In this case $S_m{}' > S_m$.

RESULTS

Calibration model

Using the NLIN procedure to fit Equation (6) to the 45 calibration SNOTEL stations required 6 iterations for the convergence criterion to be met. The results were highly significant, with an F value of 5494·45 and $p < 0·0001$. Three of the four parameters had standard errors that were less than 10% of the parameter estimate (Table I). The exception was k_1, which had a standard error that was 44% of the parameter estimate. Upper and lower confidence intervals for the four k parameters are included in Table I.

On the basis of the regression between predicted and observed values for the 45 calibration sites (Figure 5(a)), β_0 and β_1 were equal to 36·319 and 0·8381, respectively. These values were used to transform the calibration model results (Equation (9)). This resulted in a smaller intercept and a nearly one-to-one slope (22·434 and 0·9599, respectively) for the transformed *versus* observed values. Note that the transformation did not result in an intercept and slope of zero and one, respectively, because of the truncation of negative values.

The calibration model accounted for 86% of the observed variability, based on the R^2 value (Table II). The NSE for this model was 0·87, indicating high model

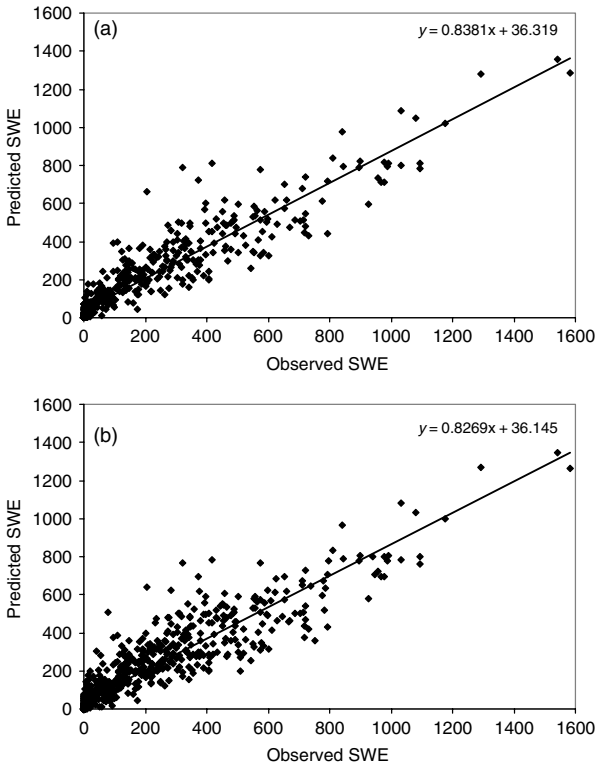

Figure 5. Predicted *versus* observed snowpack (mm of snow water equivalent) for calibration (a) and combined (b) model results. Calibration model results are for the 45 calibration sites

Table II. Evaluation of transformed snowpack models

Variable	Calibration model[a]	Validation sites[b]	Combined model[c]
R^2	0·8632	0·7638	0·8429
NSE[d]	0·8705	0·7952	0·8531
RMSE[e]	96·6717	97·3656	96·0711
RMSE/STDDEV	0·3696	0·4852	0·3961
RMSE/Range	0·0611	0·1029	0·0607
Bias[f]	15·1575	20·4945	15·7891

[a] Model parameterized using the 45 SNOTEL calibration sites (Supporting Information I) and transformed using Equation (9).
[b] Transformed calibration model results using the 25 independent SNOTEL validation sites (Supporting Information I).
[c] Model parameterized using all 70 SNOTEL sites (Supporting Information I) and transformed using Equation (9).
[d] NSE = Nash-Sutcliffe efficiency (Krause *et al*., 2005).
[e] RMSE = root mean square error = $sqrt(avg(pred - obs)^2)$. Units in mm of SWE.
[f] Bias = $avg(pred - obs)$. Units in mm of SWE.

performance. The RMSE, which is a measure of the difference between predicted and observed values, was 96·7 mm. This value was small compared with the spread and range of the observed data (RMSE/STDDEV = 0·37 and RMSE/Range = 0·06). The transformed calibration model had a bias of 15·2 mm (Table II), meaning that predicted values were, on average, somewhat higher than observed values (compared with an observed range of 0–1582 mm SWE for the 45 calibration sites).

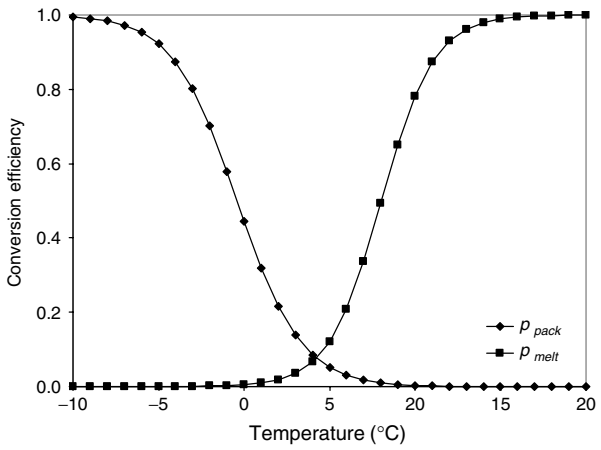

Figure 6. Conversion efficiencies for p_{pack} and p_{melt} *versus* average monthly temperature based on the combined model. Curves graphed using eqns. 3 and 5 and combined model parameter estimates from Table I

The transformed calibration model performed nearly as well when it was used to predict snowpack at the 25 validation sites (Table II). The calibration model accounted for 76% of the variability of this independent set of validation sites, which was 10% less than the calibration site value. The NSE for the validation sites was slightly lower than the calibration model (0·80 *vs* 0·87), indicating that the model performs well at predicting independent sites. RMSE was slightly higher (97·4 *vs* 96·7 mm), and the RMSE/STDDEV and RMSE/Range ratios were somewhat larger (0·49 *vs* 0·37, and 0·10 *vs* 0·06, respectively) than the corresponding values for the calibration sites. Bias was also higher (20·5 *vs* 15·2 mm for the calibration sites).

Combined model

Given that the calibration model performed well for both the calibration and independent validation sites, we re-parameterized Equation (6) using all 70 SNOTEL sites. This required 10 iterations for the NLIN procedure to converge. As was the case for the calibration model, results were highly significant (F value = 8106·52 and $p < 0·0001$). Parameter estimates for the combined model were within 2·5% of the calibration model estimates for k_2 through k_4 (Table I). In contrast, there was a 23% difference between the calibration and combined model estimates for k_1, which represents the left–right position of the snowpack conversion efficiency curve, p_{pack} (Figure 6). However, the combined model estimate for k_1 was still within the 95% confidence interval of the calibration model estimate. The standard error of k_1 was only 28% of the parameter estimate for the combined model, compared with 44% for the calibration model. Table I contains upper and lower confidence intervals for the four k parameters.

Estimates for β_0 and β_1 for the combined model (36·145 and 0·8269, respectively; Figure 5(b)) were nearly identical to the calibration model values. The intercept and slope of the transformed *versus* observed values were similarly improved (23·006 and 0·9561,

respectively). The transformed combined model and the transformed basic model performed very similarly when predicting snowpack at the 70 combined and 45 calibration sites, respectively (Table II). The transformed combined model accounted for 84% of the observed variability between the 70 combined sites, compared with an R^2 value of 0·86 for the transformed calibration model and 45 calibration sites. NSE values for the combined model were similar to the calibration model (0·85 *vs* 0·87, respectively). RMSE and RMSE/Range were slightly smaller, while RMSE/STDDEV and bias were slightly greater.

We examined mean error from the transformed combined model to see if it was influenced by elevation. Mean error is close to zero at the lowest elevations, but then rapidly increases. The highest mean error (131 mm of SWE) was observed for SNOTEL stations at elevations between 850–950 m. Mean error then declines as elevation increases to 1350 m. Between 1350 and 2150 m mean errors are relatively low (−19 to 8 mm) and vary around the zero line. Mean error then becomes more extreme (−47 to 90 mm) at elevations above 2150 m.

Since the model was fit with all monthly data combined, we also wanted to examine how error might accumulate over time. Mean error increases from nearly zero in October to a maximum of 68 mm in January. Mean error then declines and varies around the zero line between March and September. The exception is in May, when mean error increases to 27 mm.

The relationship between temperature and moisture surplus is very different for SNOTEL stations that are located <200 and ≥ 200 km from the coast. This is consistent with other studies that have classified these regions separately (McCabe and Wolock, 1999; Serreze *et al*., 1999). Compared with stations in eastern Oregon, the maritime conditions of the Cascades produce moisture surplus values that have a much greater spread, especially at lower temperatures (Figure 7(a) and (b)). This is due to the greater availability of precipitation on the coast. In spite of these different climate signatures, the model performed equally well for <200 and ≥ 200 km stations, with R^2 values of 0·83 and 0·85, respectively (compared to 0·84 for all 70 sites). NSE values for the <200 and ≥ 200 km stations did not differ from the value for combined stations (0·85). There was more of a difference in RMSE values: 117·8 and 63·3 mm for the <200 and ≥ 200 km stations, respectively. However, this was because the range in observed SWE for <200 km stations was twice that of the ≥ 200 km stations. Using the standardized RMSE/Range ratio gave equivalent values of 0·07 and 0·08, respectively (compared with 0·06 for all 70 sites). The similarity in model performance can also be seen by visually comparing observed (Figure 7(a) and (b)) *versus* modelled (Figure 7(c) and (d)) results for the <200 and ≥ 200 km stations.

Snowpack

On the basis of the results from the transformed combined model, snowpack formation is estimated to begin at the highest (i.e. coldest) peaks in the Cascades, starting in October (Figure 8). By November, the snowpack has extended throughout the higher elevations in the Cascades and is observed in the Wallowas and northeastern mountains. Snowpack continues to expand with time into lower elevation areas, reaching a maximum extent in February. At this point, much of the state has snowpack, except for the Willamette Valley and lower elevations in the Coast Range and east of the Cascades. Beginning in March, snowpack begins to recede at the lower elevations, and is absent from most of the state by June. However, snowpack accumulation continues at the highest peaks (Figure 8), reaching maximum depths in May or June. Snowpack remains at these peaks through September. Since we excluded glacial snowpack by setting initial conditions to zero, the fact that snowpack remains at the highest peaks at the end of the water year means that they would have experienced a net snowpack accumulation over this 30-year period.

The pattern of snowpack during February and March (Figure 8) closely mirrors the average annual distribution of snowfall throughout the state (Figure 4); the correlation coefficient between estimated February snowpack and average annual snowfall is 0·91. One noticeable difference is that areas that receive relatively low amounts of annual snowfall (mapped areas with snowfall of <1000 mm; Figure 4) typically do not experience snowpack accumulation (Figure 8). For example, this can be seen in the southeastern part of the state and in the area north of the Siskiyous. Most of this occurs in valleys, foothills, or low mountain areas where snowfall occurs but temperatures are not consistently low enough for seasonal snowpacks to form. These findings are similar to those of Casola *et al*. (2009), who compared SWE with inferred snowfall (calculated as the summation of precipitation occurring when daily mean temperature is $\leq 0\,^{\circ}\mathrm{C}$). They found that SWE tracked inferred snowfall well except near the base of the snowpack, where SWE values were less than inferred snowfall because of more frequent melting.

Modified surplus (S')

Statewide maps of average surplus (precipitation minus potential evapotranspiration; Figure 9) show that the entire state experiences a moisture surplus in January and a deficit during July. However, this does not account for storage of water as snowpack during the fall and winter, and release of water as snowmelt during the spring and summer. Modified surplus (Equation (11)) takes this into account, and represents the amount of available (liquid) water. Although S and S' values are similar for most of the state (Figure 9), there are significant differences at the higher peaks. On the basis of S' (Figure 9), the highest Cascade peaks and the mountainous area in the northeast all experience moisture deficits in January, since the precipitation is converted to snowpack and unavailable. In July, however, these areas and much of the high Cascades actually produce a net surplus of water

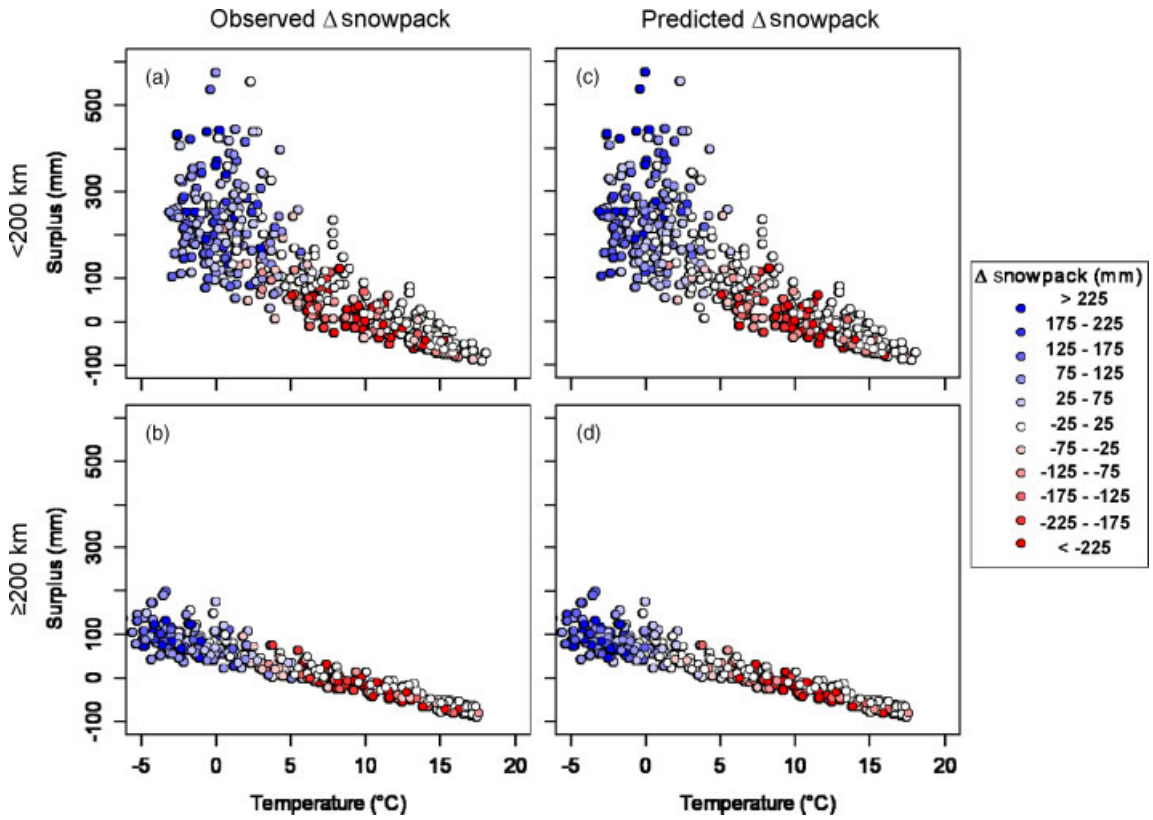

Figure 7. Relationship between temperature, surplus, and change in snowpack at SNOTEL stations <200 km (a and c) and ≥200 km (b and d) from the Oregon coast. Change in snowpack, depicted as colouring of circles, is contrasted using observed (a and b) and predicted values (c and d), with the same temperature and surplus data. Temperature and surplus values are obtained from the 400 m PRISM cell at each SNOTEL location. Each point in a plot represents an average monthly value for one SNOTEL site; there are 12 monthly points for each site

through snowmelt. These areas serve as water sources at a time when the rest of the state is experiencing moisture deficits. While the importance of snowmelt to Oregon hydrology is known (e.g. Beebee and Manga, 2004), our model allows these spatial patterns to be mapped at a high resolution.

The difference in S and S' can be further illustrated by comparing monthly values in rain- and snow-dominated basins. The Siletz River basin, located on the western slope of Oregon's Coast Range, occurs at an elevation where the dominant form of precipitation is rain. Consequently, there is little difference between monthly S and S' values, and both curves are similar in shape to actual runoff (Figure 10(a)). In comparison, the Minam River basin is located in eastern Oregon and drains the western slope of the Wallowas. Because of the high elevations, this basin receives a significant portion of its winter precipitation as snow. The monthly S' curve, which accounts for snowpack accumulation and snowmelt, accurately reflects the general shape and magnitude of the actual runoff curve, with low winter values and a June peak (Figure 10(b)). In contrast, the S curve shows maximum winter and minimum summer values.

DISCUSSION

Our objective was to develop a model that could accurately estimate long-term, average monthly snowmelt for the State of Oregon. Average (1971–2000) monthly output was required to develop a seasonality index that could be used in our Oregon hydrologic landscape classification (private communication, P.J. Wigington, Jr., US EPA Western Ecology Division, Corvallis, OR, 2 June 2011). An energy balance approach was not feasible, since this requires data (e.g. wind speed, relative humidity, solar and long-wave radiation, and ground heat flux) that are limited in their distribution or resolution. Instead, the availability of spatially extensive, high-resolution (400 m) climate data argued for a temperature index approach. The result is a nonlinear model with four parameters that control the slopes and left–right positions of the conversion curves (Equations (3) and (5) and Figure 6). The model is driven by precipitation, potential evapotranspiration, and temperature. However, PET is derived from temperature and average day length (Equations (7) and (8); Hamon, 1961), with the latter estimated from latitude. Thus, precipitation and temperature are the two primary climatic variables driving our model. The difference between precipitation and PET—moisture surplus—determines the amount of water that is potentially available from climatic input. Temperature serves the dual role of controlling the movement of precipitation into and out of storage through snowpack formation and snowmelt.

When parameterized with 45 calibration sites, our model accurately estimated snowmelt at 25 independent

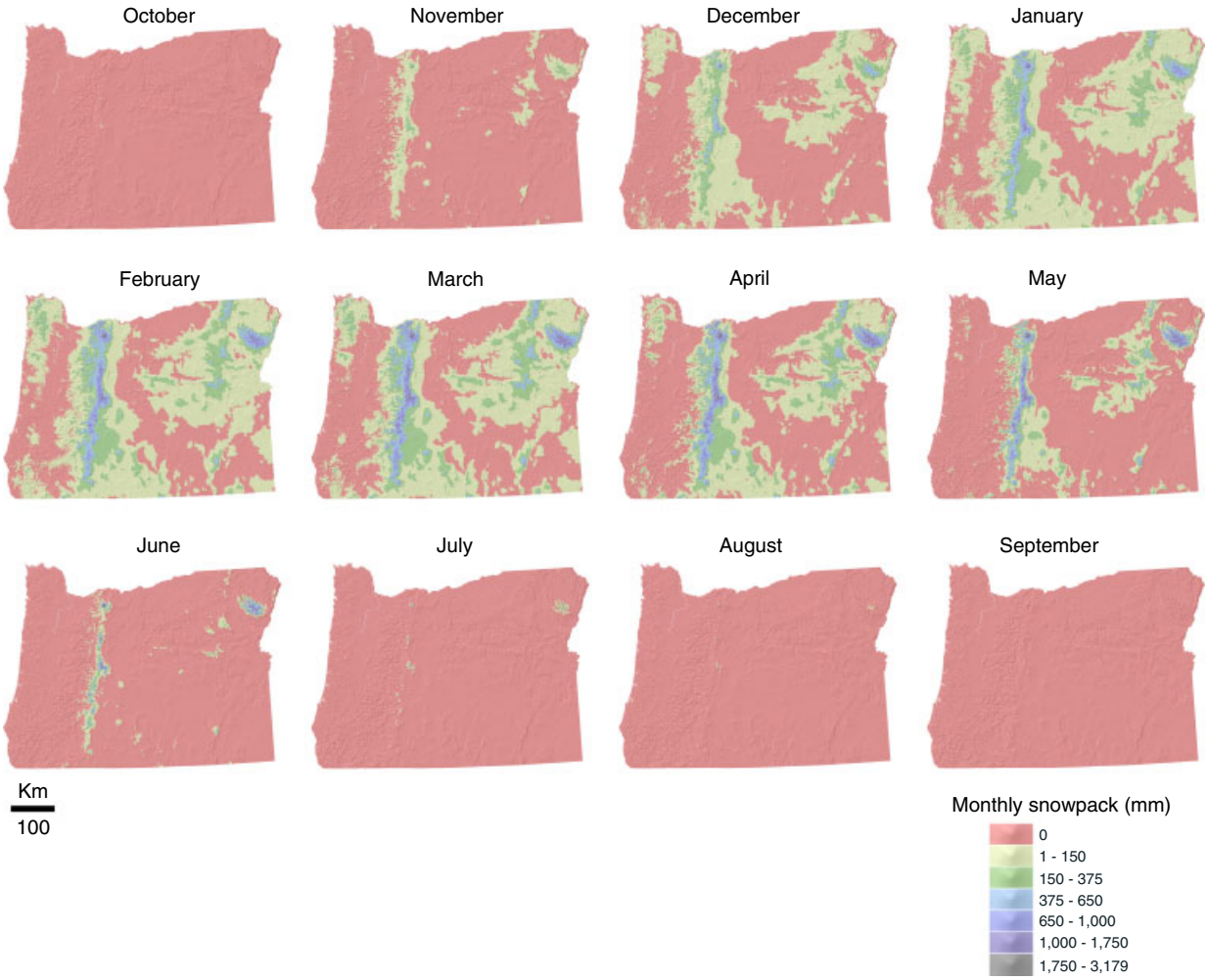

Figure 8. Predicted average monthly snowpack ($PACK_m^*$) for Oregon

validation sites ($R^2 = 76\%$, and NSE = 0·80; Table II). The model also works equally well for two regions (<200 and ≥200 km from the coast) having very different temperature-surplus relationships (Figure 7). These results seem to contradict the assertion that temperature index models cannot be applied to heterogeneous terrain or transferred to basins with different climatic conditions (Williams and Tarboton, 1999).

Snow accumulation can be estimated from ground surveys, aerial photography, or satellite imagery (Martinec and Rango, 1986; Kustas *et al*., 1994; Cline *et al*., 1998; Martinec *et al*., 2008; Singh *et al*., 2009). Alternatively, snow accumulation can be modelled as a function of precipitation and air temperature. This has been done using a binary step function (Fontaine *et al*., 2002; Martinec *et al*., 2008) or a linear threshold (Tarboton *et al*., 1995; McCabe and Wolock, 1999). For this study, we used an S-shaped, inverted logistic function (Equation (3)). Other researchers have observed a similar relationship between temperature and the percent of precipitation occurring as snow. Auer (1974) classified about 1000 US precipitation observations as rain or snow. He found that the probability that precipitation occurred as snow was asymptotic, and had the same general shape as our snowpack conversion efficiency function, p_{pack} (Figure 6). More recently, Bartlett *et al*. (2006) examined 10 years of hourly meteorological data from 39 stations in Canada. Their results were similar to Auer's except their curve—which included mixed snow and freezing precipitation—was shifted to the left by about a degree (Bartlett *et al*., 2006). The reverse S-shaped curve can also describe the relationship between temperature and the ratio of monthly snowfall to precipitation. Beschta (1975) observed such a relationship for climate stations in Alaska, Minnesota, and Montana. However, the best fit relationships were quadratic for stations in Oregon, Arizona, and New England. Beschta (1975) hypothesized that all sites would have had the S-shaped relationship if the data had spanned the full range of temperature and snowfall ratio values. An S-shaped, inverted logistic function similar to ours has also been used to model snow conversion efficiency at the Hitsujigaoka study site in Japan (Rutter *et al*., 2009).

Our snowpack conversion efficiency curve (Figure 6) is shifted further to the left and more stretched (i.e. is less steep) than results from Auer (1974) and Bartlett *et al*. (2006). For example, our analysis shows 5, 50, and 95% conversion to snowpack at surface temperatures of 5·1, −0·4, and −5·9 °C, respectively. Corresponding

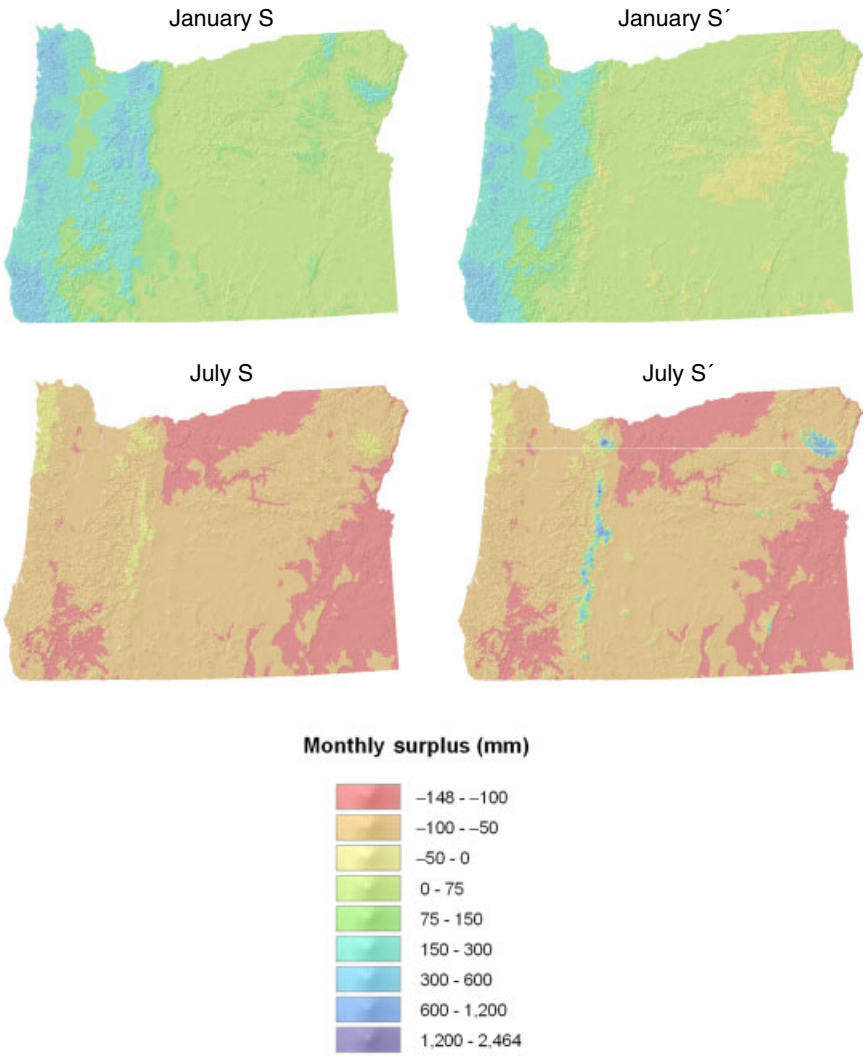

Figure 9. Comparison of average surplus (S) and modified surplus (S') values in Oregon for January and July. Modified surplus represents the average monthly amount of available (liquid) water

temperatures for Auer (1974) were 5·6, 2·5, and 1·1 °C, respectively. One possible reason for this difference is that the ordinate in our plot is the ratio of snowpack to moisture surplus (Figure 6), rather than the ratio of snow to precipitation events (Auer, 1974; Bartlett *et al*., 2006). Net snowpack formation is a more complex process than the occurrence of snowfall. It depends not only on the amount of snowfall, but also on factors such as canopy interception, wind dispersion, and ground temperature. As a result, converting precipitation to snowpack may require lower temperatures than are associated with snowfall events. However, we believe the main reason why our curve is shifted towards colder temperatures is that we use monthly data, rather than instantaneous or hourly values. A month with below-freezing average temperature can still experience significant rainfall if the precipitation falls on days with above-freezing temperatures. Thus, a lower average temperature is required for a given conversion rate when integrating over a longer time period. The curves in Beschta's (1975) analysis, which were also based on monthly values, were similarly shifted towards colder temperatures.

Energy balance approaches model snowmelt by simulating the physical processes that affect heat and water balances. In contrast, temperature index approaches estimate snow accumulation as a function of air temperature (Martinec and Rango, 1986; Kustas *et al*., 1994; McCabe and Wolock, 1999; Martinec *et al*., 2008; Singh *et al*., 2009). For example, the Snowmelt Runoff Model (SRM) (Martinec and Rango, 1986; Martinec *et al*., 2008) calculates a snowmelt rate (cm day^{-1}) as the product of the number of degree-days above freezing and a degree-day factor that represents the snowmelt depth per degree-day. The degree-day factor is not constant, but is a function of snow density, which varies temporally and spatially to reflect the age and condition of the snowpack. Fontaine *et al*. (2002) explicitly incorporate this temporal variability in the SWAT model by defining their melt coefficient as a sine function of the day of year. Our method differs from SRM and other degree-day approaches in that our melt factor, p_{melt}, is a proportion rather than a depth. Also, in our formulation the effect of temperature is S-shaped, rather than linear.

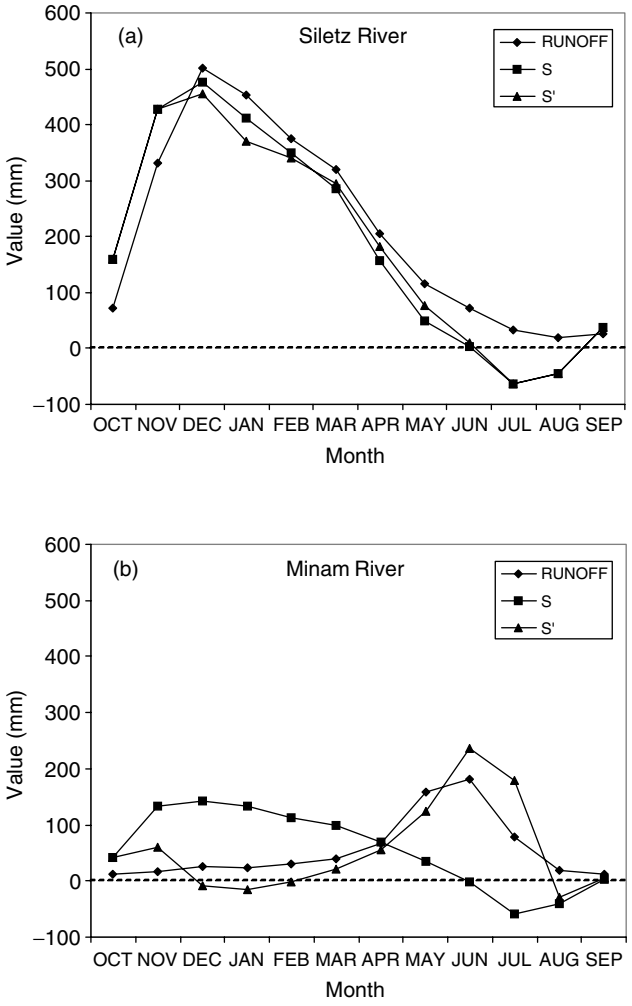

Figure 10. Comparison of monthly average surplus (S), modified surplus (S'), and runoff values for (a) the rain-dominated Siletz River, Oregon (USGS site #14305500) and (b) the snowmelt-dominated Minam River, Oregon (USGS site #13331500). S and S' values are averages for all 400 m cells within each basin. Runoff calculated from 1971–2000 average monthly discharge data from US Geological Survey National Water Information System (http://waterdata.usgs.gov/or/nwis/dv/?referred_module=sw; accessed Sept. 14, 2009)

We cannot directly compare the performance of our model with other temperature index approaches, because those models typically have a finer temporal resolution than ours (daily *vs* long-term monthly averages). Still, a comparison can be informative because we should be able to predict 30-year monthly averages more accurately than daily values. Kustas *et al.* (1994) report R^2 values of 0·54 and 0·73 for a temperature index and modified temperature index approach, respectively. In a study by Singh *et al.* (2009), R^2 values for annual runs of a temperature index model ranged from 0·01 to 0·46, with a modified temperature index model generally performing better (R^2 range from 0 to 0·87). On the basis of 86 applications of SRM from around the world (Martinec *et al.*, 2008), R^2 values ranged from 0·42 to 0·97, with 70% of them having R^2 values better than our validation value of 0·76 (Table II). While our model compares favourably with the studies by Kustas *et al.* (1994) and Singh *et al.* (2009), it does not typically perform as well as SRM, even though we are predicting monthly averages. However, most of these analyses were calibrated to small study areas that represent less geographic variability: 50% of the 86 SRM applications had surface areas $\leq$700 km^2, and 87% of them were $\leq$10000 km^2. In contrast, we calibrated and tested our model using 70 stations from around the state of Oregon, which has an area of 251165 km^2 and varies in climate from very wet to arid. Thus, we are able to estimate long-term snowmelt averages over a large, heterogeneous area with reasonable accuracy.

Our modelling approach is similar to that of McCabe and Wolock (1999), who examine the effects of climate change on snowpack in the western US. They develop a simple temperature index approach that models snowpack formation and snowmelt. As with our approach, they define conversion rates for snowpack and snowmelt as functions of temperature. However, they use linear, rather than S-shaped, relationships to describe these temperature effects. McCabe and Wolock (1999) use their model to estimate snowpack between 1948 and 1987 for 4 regional clusters in the western US. R^2 and RMSE values for the Pacific Northwest cluster (which includes stations from Oregon, Washington, Idaho, and Montana) were 0·75 and 101 mm, respectively, compared to 0·84 and 96 mm for our combined model (Table II).

Although the approaches are similar, there are a number of differences between our model and the one developed by McCabe and Wolock (1999), besides their use of linear temperature functions. These authors utilize the same upper and lower temperature thresholds for snow accumulation and snowmelt, while we use two separate curves (Figure 6). Our snowpack curve is shifted to the left compared with theirs: for our model, conversion rates for precipitation into snow are 45 and 5% at 0 and 5 °C, respectively, compared to their rates of 100 and 0%. On the other hand, our snowmelt curve is shifted to the right, with rates of 1 and 12% at 0 and 5 °C, respectively, compared with their rates of 0 and 50%. In addition, they limit the maximum snowmelt rate to 50% and convert all snowpack $\leq$10 mm to snowmelt; we do neither of these. McCabe and Wolock (1999) use April 1 snowpack values to assess the accuracy of their model, while we use monthly data over the entire year. Also, their study area includes stations over 10 western states, while our analysis is limited to Oregon.

The methodological differences just described are not too significant. However, there are two other factors that distinguish our approach from McCabe and Wolock's (1999) work, and from other snowmelt models. First, our snowpack estimates are thirty-year monthly means, and so eliminate daily and inter-annual variability which other models work to represent. Use of monthly mean temperature should remove local biases (Beniston *et al.*, 2003) and average out the effects of transitory threshold phenomena, such as sub-freezing rain or above-freezing snow (Nolin and Daly, 2006). Also, a comparison of 33 snowmelt models at 5 locations found that events where air temperature exceeded 0 °C for more than

two consecutive days had the greatest effect on model divergence (Rutter *et al*., 2009). Use of monthly averages could reduce or eliminate such effects. The use of monthly averages is possible because our objectives focus on long-term trends.

Second, we apply our calibrated model statewide using the high resolution PRISM data. Such spatially detailed estimates do not exist over extensive areas. For example, Nolin *et al*. (in press) point out that accurate basin-wide measurements of snowpack are not available for the Oregon Cascades. However, they note that there is a critical need for such data to forecast water supply and demand at the watershed scale, since this is where these resources are managed. Given that PRISM data are available for the entire US, it may be possible to use our approach to provide accurate estimates of long-term snowmelt nationally. From this perspective, it is especially promising that our model performed equally well for two very different climate regimes (Figure 7). However, the method should be tested in other climatic regions before it is applied nationally.

Caveats

While the results of our model are encouraging, there are a number of limitations that need to be kept in mind. First, we specifically modelled 30-year monthly averages for our Hydrologic Landscape application. This means it is not appropriate to use this model to predict monthly values for a specific year. Also, the model cannot be used to provide information on changes in synoptic-scale phenomena, such as dates of peak runoff, winter thaw events, or annual maximum snow loads.

Our model only tracks snowpack and snowmelt resulting from monthly moisture inputs; any snowmelt from glacial snowpack caused by regional warming—due to global climate change or variations in climate patterns such as the PDO or the NPI (Beebee and Manga, 2004; Mote, 2006)—would not be accounted for.

Results and trends from climate studies can be sensitive to the period of record chosen for analysis. Casola *et al*. (2009) point out that historic snowpack data in the Pacific Northwest are correlated with the NPI, which is an indicator of the amplitude and polarity of the PDO. NPI and average SWE values were greater during the period from the 1940s to the mid-1970s, compared with values from 1977 onward. Our model reflects the relatively dry period that occurred during much of 1971–2000 due to this regime shift. As noted by Cline *et al*. (1998), results from empirically derived models such as ours may not be valid for periods with different conditions.

Another issue is that our model assumes that there is no net movement of snow between cells, and that snowpack accumulates in place. Snowpack would be overestimated in source areas where snow is removed by wind or avalanches, and underestimated in sink areas where there is net snow deposition. Such an underestimate was observed at a study site in the Sierra Nevada that included an area where heavy snow accumulation occurred, due in part to a leeward slope orientation and avalanche redeposition (Molotch *et al*., 2004). In addition, our model would not capture changes in snowmelt due to differences in solar radiation between north- and south-facing slopes. Thus, caution should be used in interpreting model results for individual cells. A more appropriate use of the model would be to aggregate results over large enough areas that net snow movement is not significant and aspect differences are averaged out.

Errors in the PRISM-derived independent variables could also affect our results. PRISM climate data have been shown to perform as well as or outperform other climate data, such as Daymet and WorldClim (Daly *et al*., 2008). For example, 800 m PRISM data did a better job than these two datasets at portraying spatial patterns in estimated runoff for six basins in Washington's Olympic Mountains. For the eastern and central US, averages of monthly results have relatively low mean absolute error values of 4·7–6·8 mm, 0·6–0·8 °C, and 0·4–0·6 °C for precipitation, minimum temperature, and maximum temperature, respectively (Daly *et al*., 2008). The western US had higher errors, though, with values of 6·1–8·2 mm, 1·2 °C, and 0·7 °C, respectively. However, the largest errors occurred in coastal areas and the mountainous west, including portions of Oregon. Also, downscaling the 800 m PRISM data to the 400 m resolution that we used would introduce additional error. In spite of this, we found that we could accurately model snowpack at SNOTEL stations using these PRISM data. The relative spatial and temporal trends contained in the PRISM data are apparently adequate for this purpose.

Issues with the SNOTEL data are potentially more serious. There are a number of possible sources of error and biases in these data that could affect how accurately they represent spatial patterns in snowpack during the 1971–2000 period. First, we noted in the methods section that monthly values are estimated by averaging snowpack data from the 1st and 15th day of each month. We also pointed out that none of the 70 stations that we used in our analysis were operating for the entire period from 1971 to 2000 (Supporting Information I). Also, the type of snow pillow used for data collection was switched at 30 of the SNOTEL stations, from steel to hypalon or vice versa (Supporting Information I). This has been suggested to cause a bias in observed snow accumulation (Julander and Bricco, 2006; Julander 2007). However, we found no evidence of such a bias in an examination of 10 Oregon SNOTEL stations that had data from steel and hypalon pillows as well as independently collected data from a nearby snow course (Supporting Information II).

Another issue with SNOTEL stations is that they are not representative of the entire state. Areas in the Coast Range and Klamath Mountains (Figure 1) are underrepresented or not represented at all by SNOTEL sites (Figure 4). Also, SNOTEL stations occur in small flat clearings and so are not representative of forested, sloped areas (Brown, 2009). SNOTEL data also have elevational biases, although coverage of lower and moderate elevations is considered to be better in the Pacific Northwest

(Grundstein and Mote, 2010). Yet, in an analysis of a basin in the Oregon Cascades, Brown (2009) found gaps in SNOTEL coverage at low and high elevations: the elevation range for snow was 1000–3000 m, compared to a narrower range of 1200–1500 m for SNOTEL stations. Statewide, Oregon SNOTEL stations range in elevation from 628 to 2411 m (Supporting Information I), while maximum elevation is 3426 m at Mt Hood. On the basis of our analysis, this elevational bias does not appear to be an issue at lower elevations, but it could cause greater uncertainty at higher elevations.

It would be desirable to have an independent dataset that could be used to assess how well our model performed outside the SNOTEL elevational range. However, choices for this are limited. For example, the map in Figure 4 shows snowfall, not snowpack, is based on a different 30-year period (1961–1990), and is itself model based. Satellite-based snow coverage would also be inappropriate, both because of differences between snow coverage and snowpack, and because our estimates are 30-year monthly averages. Datasets from individual sites have been used to test and compare models that are calibrated with time series data having daily or shorter time steps (WMO, 1986; Rutter *et al*., 2009). However, this method would not work for a spatially extensive approach such as ours that uses multiple sites for calibration. One dataset that the model should be tested against is the network of cooperative observation stations, since these stations have a larger elevational range than SNOTEL stations (Grundstein and Mote, 2010). In spite of all these limitations, SNOTEL data are the most comprehensive and extensive dataset available in the western US for calibrating a temperature index model. They can function as a useful approximate metric for snowpack (Nolin *et al*., in press). Expanding SNOTEL stations to include a wider range of elevations would improve the utility of these data for applications such as ours.

Although overall error for our model is low (Table II), mean errors at elevations near 1000 m are relatively high (up to 131 mm). This could be especially significant for areas, like the Cascades, where maritime snow falls at lower elevations with relatively warm temperatures (Nolin and Daly, 2006). However, we believe that our model is useful for objectives such as ours. For example, our analysis of the Minam basin (Figure 10(b)) demonstrates that S' values derived with our model (Equation (11)) and integrated over a 622 km^2 watershed can accurately reflect the overall pattern and magnitude of actual runoff in a snow-dominated basin. We have used a similar approach to conduct an analysis of the Minam and 29 other Oregon basins having runoff data for 1971–2000 (private communication, P.J. Wigington, Jr., US EPA Western Ecology Division, Corvallis, OR, 2 June 2011). In that study, we compare runoff with S^*, which is a version of S' that is constrained to non-negative values. We find many instances where S^* values match the pattern and magnitude of basin runoff. For cases where the curves diverge, we hypothesize (private communication, P.J. Wigington, Jr., US EPA Western Ecology Division, Corvallis, OR, 2 June 2011) that the differences could represent (1) errors in the way that we combine S^* across basins, (2) seasonal changes in soil storage, or (3) losses or gains from outside the basin.

Our model may also be useful for investigating the impacts of climate change on regional hydrology. For example, we plan to run our model using temperature and precipitation data derived from global climate change models to compare snowpack between 1971–2000 and 2041–2070. However, such an assessment assumes that the empirical relationships that we observed for the 1971–2000 period will be equally valid under future climate conditions. If the empirical factors that are depicted in our conversion efficiency curves (Figure 6) continue to hold, then an increase in temperature from 0 to 2 °C would cause the proportion of precipitation converted to snowpack to be halved from 0·44 to 0·22. The same temperature change would also cause an increase in snowmelt conversion, from 0·005 to 0·019. Although this change is small in magnitude, it represents an almost fourfold increase in the snowmelt rate. The relative magnitude of these changes is consistent with results from Casola *et al*. (2009), who conclude that the direct effect of temperature change is primarily due to a shift from snow to rain, and that increased melting plays a lesser role. However, increased temperature can also have an indirect effect by increasing precipitation rates at high elevations (Beniston *et al*., 2003). Use of our model with temperature and precipitation data from global climate change models will allow us to further investigate these effects.

SUMMARY AND CONCLUSIONS

We developed an empirical nonlinear model to predict snowpack and snowmelt in Oregon. The two primary climatic variables that drive the model are precipitation and temperature. Although it shares some characteristics with other models, our approach is distinguished by our objective to make accurate and high resolution statewide estimates of long-term mean monthly snowpack.

We calibrated the model using snowpack data from 45 SNOTEL sites in Oregon and 400 m climate data from PRISM. Despite the fact that PRISM data have higher errors in the mountainous west and coastal areas (Daly *et al*., 2008), the fit model accurately estimated snowpack at 25 independent validation sites ($R^2 = 76\%$, NSE $= 0{\cdot}80$; Table II). Calibrating the model with data from all 70 SNOTEL sites resulted in a combined model that explained 84% of the variation in monthly snowpack. Model performance was the same for SNOTEL sites <200 and ≥ 200 km from the coast, in spite of major differences in temperature-surplus relationships (Figure 7). This suggests that the model is robust with respect to different climatic conditions, irrespective of the comment that empirical models cannot be transferred to basins with different climatic conditions (Williams and Tarboton, 1999). Despite biases in the SNOTEL data, modified surplus values derived with our model matched actual runoff

data at a snow-dominated basin. Our model should be especially useful for making regional hydrological comparisons across basins that are differentially affected by snowpack (e.g. precipitation- *vs* snow-dominated areas) and may be useful for investigating the hydrologic impacts of climate change at similar scales. Future expansion of Hydrologic Landscape mapping into Washington and Idaho will allow the model to be tested over a wider range of climatic and physiographic conditions.

ACKNOWLEDGMENTS

We gratefully acknowledge John Van Sickle and E. Henry Lee, both of EPA's Western Ecology Division, for their input on the modelling and statistical analysis. We also thank David DeWalle, Gregory McCabe, Sarah Lewis, and three anonymous reviewers for helpful comments on earlier drafts. The information in this document has been funded entirely by the US EPA, and has been subjected to EPA's peer and administrative review and approved for publication as an EPA document. Mention of trade names or commercial products does not constitute endorsement or recommendation for use.

REFERENCES

Adam JC, Hamlet AF, Lettenmaier DP. 2009. Implications of global climate change for snowmelt hydrology in the twenty-first century. *Hydrological Processes* **23**: 962–972.

Albert M, Krajeski G. 1998. A fast, physically based point snowmelt model for use in distributed applications. *Hydrological Processes* **12**: 1809–1824.

Auer AH Jr. 1974. The rain versus snow threshold temperatures. *Weatherwise* **27**: 67.

Barnett TP, Pierce DW, Hidalgo HG, Bonfils C, Santer BD, Das T, Bala G, Wood AW, Nozawa T, Mirin AA, Cayan DR, Dettinger MD. 2008. Human-induced changes in the hydrology of the western United States. *Science* **319**: 1080–1083.

Bartlett PA, MacKay MD, Verseghy DL. 2006. Modified snow algorithms in the Canadian Land Surface Scheme: Model runs and sensitivity analysis at three boreal forest stands. *Atmosphere-Ocean* **43**: 207–222.

Beebee RA, Manga M. 2004. Variation in the relationship between snowmelt runoff in Oregon and ENSO and PDO. *Journal of the American Water Resources Association* **40**: 1011–1024.

Beniston M, Keller F, Goyette S. 2003. Snow pack in the Swiss Alps under changing climatic conditions: an empirical approach for climate impact studies. *Theoretical and Applied Climatology* **74**: 19–31.

Beschta RL. 1975. A method for estimating snowfall amounts. *Water Resources Bulletin* **11**: 1209–1219.

Brown AL. 2009. Understanding the impact of climate change on snowpack extent and measurement in the Columbia River Basin and nested sub basins. MS Thesis, Dept. of Geosciences, Oregon State Univeristy, Corvallis, OR.

Carroll T, Cline D, Olheiser C, Rost A, Nilsson A, Fall G, Bovitz C, Li L. 2006. NOAA's national snow analyses. Proceedings of the 74th Annual Meeting of the Western Snow Conference, Las Cruces, NM, April 17–20, 2006. Available online at http://www.nohrsc.nws.gov/technology/pdf/WSC_2006.pdf.

Casola JH, Cuo L, Livneh B, Lettenmaier DP, Stoelinga MT, Mote PW, Wallace JM. 2009. Assessing the impacts of global warming on snowpack in the Washington Cascades. *Journal of Climate* **22**: 2758–2772.

Church MR, Bishop GD, Cassell DL. 1995. Maps of regional evapotranspiration and runoff/precipitation ratios in the northeast United States. *Journal of Hydrology* **168**: 283–298.

Cline D, Elder K, Bales R. 1998. Scale effects in a distributed snow water equivalence and snowmelt model for mountain basins. *Hydrological Processes* **12**: 1527–1536.

Dahl M, Nilsson B, Langhoff JH, Refsgaard JC. 2007. Review of classification systems and new multi-scale typology of groundwater-surface water interaction. *Journal of Hydrology* **344**: 1–16.

Daly C, Halbleib M, Smith JI, Gibson WP, Doggett MK, Taylor GH, Curtis J, Pasteris PP. 2008. Physiographically sensitive mapping of climatological temperature and precipitation across the conterminous United States. *International Journal of Climatology* **28**: 2031–2064.

Devito K, Creed I, Gan T, Mendoza C, Petrone R, Silins U, Smerdon B. 2005. A framework for broad-scale classification of hydrologic response units on the Boreal Plain: is topography the last thing to consider? *Hydrological Processes* **19**: 1705–1714.

Fontaine TA, Cruickshank TS, Arnold JG, Hotchkiss RH. 2002. Development of a snowfall-snowmelt routine for mountainous terrain for the soil water assessment tool (SWAT). *Journal of Hydrology* **262**: 209–223.

Grundstein A, Mote TL. 2010. Trends in average snow depth across the western United States. *Physical Geography* **31**: 172–185.

Hamlet AF, Mote PW, Clark MP, Lettenmaier DP. 2005. Effects of temperature and precipitation variability on snowpack trends in the western United States. *Journal of Climate* **18**: 4545–4561.

Hamon WR. 1961. Estimating potential evapotranspiration. *Journal of Hydraulics Division, Proceedings of the American Society of Civil Engineers* **87**: 107–120.

Hijmans RJ, Cameron SE, Parra JL, Jones PG, Jarvis A. 2005. Very high resolution interpolated climate surfaces for global land areas. *International Journal of Climatology* **25**: 1965–1978.

Holmes MGR, Young AR, Gustard A, Grew R. 2002. A region of influence approach to predicting flow duration curves within ungauged catchments. *Hydrology and Earth System Sciences* **6**: 721–731.

Howat IM, Tulaczyk S. 2005. Climate sensitivity of spring snowpack in the Sierra Nevada. *Journal of Geophysical Research* **110**: F04021, DOI:10.1029/2005JF000356.

Hutchinson KJ, Haynes DA, Schnoor JL. 2010. Human-impacted water resources: domain stratification and mapping to determine hydrologically similar units. *Environmental Science and Technology* **44**: 7890–7896.

Julander RP. 2007. Soil surface temperature difference between steel and hypalon pillows. Paper presented at the 75th Annual Meeting of the Western Snow Conference, Kailua-Kona, HI, April 16–19, 2007. Available online at http://www.ut.nrcs.usda.gov/snow/siteinfo/data_bias/soiltemps-steelandhypalon.pdf.

Julander RP, Bricco M. 2006. An examination of external influences imbedded in the historical snow data of Utah. All US Government Documents (Utah Regional Depository), Paper 116. Available online at http://digitalcommons.usu.edu/govdocs/116/.

Knowles N, Dettinger MD, Cayan DR. 2006. Trends in snowfall versus rainfall in the western United States. *Journal of Climate* **29**: 4545–4559.

Kolditz O, Du Y, Bürger C, Delfs J, Kuntz D, Beinhorn M, Hess M, Wang W, van der Grift B, te Stroet C. 2007. Development of a regional hydrologic soil model and application to the Beerze-Reusel drainage basin. *Environmental Pollution* **148**: 855–866.

Krause P, Boyle DP, Bäse F. 2005. Comparison of different efficiency criteria for hydrological model assessment. *Advances in Geosciences* **5**: 89–97.

Kroll C, Luz J, Allen B, Vogel RM. 2004. Developing a watershed characteristics database to improve low streamflow prediction. *Journal of Hydrologic Engineering* **9**: 116–125.

Kustas WP, Rango A, Uijlenhoet R. 1994. A simple energy budget algorithm for the snowmelt runoff model. *Water Resources Research* **30**: 1515–1527.

Leibowitz SG, Wigington PJ Jr, Rains MC, Downing DM. 2008. Non-navigable streams and adjacent wetlands: addressing science needs following the Supreme Court's *Rapanos* decision. *Frontiers in Ecology and the Environment* **6**: 364–371.

Liang XU, Lettenmaier DP, Wood EF, Burges SJ. 1994. A simple hydrologically based model of land surface water and energy fluxes for general circulation models. *Journal of Geophysical Research* **99**(D7): 14415–14428.

Lu J, Sun G, McNulty SG, Amatya DM. 2005. A comparison of six potential evapotranspiration methods for regional use in the southeastern United States. *Journal of the American Water Resources Association* **41**: 621–633.

Lydolph PE. 1985. *The Climate of the Earth*. Rowman and Allanheld: Totowa, NJ.

Martinec J, Rango A. 1986. Parameter values for snowmelt runoff modeling. *Journal of Hydrology* **84**: 197–219.

Martinec J, Rango A, Roberts R. 2008. Snowmelt Runoff Model (SRM) User's Manual. WinSRM Version 1.11. Agricultural Experiment

Station Special Report 100, New Mexico State University, Las Cruces, NM.

McCabe GJ, Wolock DM. 1999. General-circulation-model simulations of future snowpack in the western United States. *Journal of the American Water Resources Association* **35**: 1473–1484.

McDonnell JJ, Woods R. 2004. On the need for catchment classification. *Journal of Hydrology* **299**: 2–3.

Molotch NP, Painter TH, Bales RC, Dozier J. 2004. Incorporating remotely-sensed snow albedo into a spatially-distributed snowmelt model. *Geophysical Research Letters* **31**: L03501, DOI:10.1029/2003GL019063.

Mote PW. 2006. Climate-driven variability and trends in mountain snowpack in western North America. *Journal of Climate* **19**: 6209–6220.

National Water and Climate Center (NWCC). 2009. *SNOTEL and snow survey and water supply forecasting*. US Department of Agriculture, Natural Resources Conservation Service. Available online at http://www.wcc.nrcs.usda.gov/snotel/SNOTEL-brochure.pdf.

Nolin AW, Daly C. 2006. Mapping "at risk" snow in the Pacific Northwest. *Journal of Hydrometeorology* **7**: 1164–1171.

Nolin AW, Sproles E, Brown A. Climate change impacts on snow and water resources in the Columbia, Willamette, and McKenzie River Basins, USA: A nested watershed study. Part II, Chapter 2, in *Transboundary River Governance in the Face of Uncertainty: The Columbia River Treaty*, Cosens B (ed). OSU Press: Corvallis, OR (in press).

Oudin L, Hervieu F, Michel C, Perrin C, Andréassian V, Anctil F, Loumagne C. 2005. Which potential evapotranspiration input for a lumped rainfall-runoff model? Part 2—Towards a simple and efficient potential evapotranspiration model for rainfall-runoff modelling. *Journal of Hydrology* **303**: 290–306.

Rosenberry DO, Stannard DI, Winter TC, Martinez ML. 2004. Comparison of 13 equations for determining evapotranspiration from a prairie wetland, Cottonwood Lake area, North Dakota, USA. *Wetlands* **24**: 483–497.

Ruffner JA (ed). 1985. *Climates of the States: National Oceanic and Atmospheric Administration Narrative Summaries, Tables and Maps for Each State with Overview of State Climatologist Programs*, 3rd edn. Gale Research Co.: Detroit, MI. Available online at http://www.wrcc.dri.edu/narratives/OREGON.htm.

Rutter N, Essery R, Pomeroy J, Altimir N, Andreadis K, Baker I, Barr A, Bartlett P, Boone A, Deng H, Douville H, Dutra E, Elder K, Ellis C, Feng X, Gelfan A, Goodbody A, Gusev Y, Gustafsson D, Hellström R, Hirabayashi Y, Hirota T, Jonas T, Koren V, Kuragina A, Lettenmaier D, Li W-P, Luce C, Martin E, Nasonova O, Pumpanen J, Pyles RD, Samuelsson P, Sandells M, Schädler G, Shmakin A, Smirnova TG, Stähli M, Stöckli R, Strasser U, Su H, Suzuki K, Takata K, Tanaka K, Thompson E, Vesala T, Viterbo P, Wiltshire A, Xia K, Xue Y, Yamazaki T. 2009. Evaluation of forest snow processes models (SnowMIP2). *Journal of Geophysical Research* **114**: D06111, DOI:10.1029/2008JD011063.

Sanborn SC, Bledsoe BP. 2006. Predicting streamflow regime metrics for ungauged streams in Colorado, Washington, and Oregon. *Journal of Hydrology* **325**: 241–261.

Santhi C, Kannan N, Arnold JG, Di Luzio M. 2008. Spatial calibration and temporal validation of flow for regional scale hydrologic modeling. *Journal of the American Water Resources Association* **44**: 829–846.

SAS Institute. 2003. *SAS OnlineDoc 9·1 for the Web*. SAS Publishing: Cary, NC. Available online at http://support.sas.com/91doc/docMain page.jsp.

Serreze MC, Clark MP, Armstrong RL, McGinnis DA, Pulwarty RS. 1999. Characteristics of the western United States snowpack from snowpack telemetry (SNOTEL) data. *Water Resources Research* **35**: 2145–2160.

Singh PR, Gan TY, Gobena AK. 2009. Evaluating a hierarchy of snowmelt models at a watershed in the Canadian Prairies. *Journal of Geophysical Research* **114**: D04109, DOI:10.1029/2008JD010597.

Sivapalan M. 2005. Pattern, process, and functions: Elements of a unified theory of hydrology at the catchment scale. In *Encyclopedia of Hydrological Sciences*, Anderson MG, McDonnell JJ (eds). John Wiley and Sons: New York.

Sobota DJ, Harrison JA, Dahlgren RA. 2009. Influences of climate, hydrology, and land use on input and export of nitrogen in California watersheds. *Biogeochemistry* **94**: 43–62.

Tarboton DG, Chowdhury TG, Jackson TH. 1995. A spatially distributed energy balance snowmelt model. In *Biogeochemistry of Seasonally Snow-Covered Catchments, IAHS Publ.,* **228**: 141–155.

Taylor GH, Hannan C. 1999. *The Climate of Oregon: From Rain Forest to Desert*. Oregon State University Press: Corvallis, OR.

Thornton PE, Running SW, White MA. 1997. Generating surfaces of daily meteorological variables over large regions of complex terrain. *Journal of Hydrology* **190**: 214–251.

Vogel RM, Wilson I, Daly C. 1999. Regional regression models of annual streamflow for the United States. *Journal of Irrigation and Drainage Engineering* **125**: 148–157.

Williams KS, Tarboton DG. 1999. The ABC's of snowmelt: a topographically factorized energy component snowmelt model. *Hydrological Processes* **13**: 1905–1920.

Winter TC. 2001. The concept of hydrologic landscapes. *Journal of the American Water Resources Association* **37**: 335–349.

Wolock DM, Winter TC, McMahon G. 2004. Delineation and evaluation of hydrologic-landscape regions in the United States using Geographic Information System tools and multivariate statistical analyses. *Environmental Management* **34**(Suppl. 1): S71–S88.

World Meteorological Organization (WMO). 1986. Results of an intercomparison of models of snowmelt runoff. In *Modelling Snowmelt-Induced Processes, IAHS Publ.,* **155**: 103–112.

Xu C-Y, Singh VP. 2001. Evaluation and generalization of temperature-based methods for calculating evaporation. *Hydrological Processes* **15**: 305–319.